

Erastin-like anti-Warburg compounds X1 and X4 are GLS2-selective covalent glutaminase inhibitors

Cléa S. Crane², Morgan P. Miele¹, Ranjini Iyengar¹, Noah P. Strathmann¹, Sainabou Jallow¹,
Scott M. Ulrich^{1*}

¹ *Department of Chemistry, Ithaca College, Ithaca, NY 14850, USA*

² *Department of Chemistry and Chemical Biology, Cornell University, Ithaca, NY 14850, USA*

* Corresponding author. Email: sulrich@ithaca.edu

Abstract

The Warburg effect is a metabolic alteration in cancer cells characterized by aerobic glycolysis and lactate production. A recent phenotypic screen for compounds that reverse Warburg metabolism identified two compounds, X1 and X4, that restore the mitochondrial membrane potential, decrease lactate production, and increase the level of reactive oxygen species in cancer cells. Here we show that X1 and X4 are GLS2-selective covalent glutaminase inhibitors. Glutaminase enzymes hydrolyze glutamine to glutamate, which supports cancer cell metabolism through TCA cycle anaplerosis and glutathione biosynthesis. The GLS1 glutaminase isozyme has well-established roles in cancer cell metabolism. Conversely, GLS2 is an enigmatic enzyme with reported roles in both tumor promotion and tumor suppression and remains an underdeveloped drug target. This finding suggests roles for GLS2 in supporting Warburg metabolism and managing oxidative stress in cancer cells. X1 and X4 may accelerate the development of high-quality inhibitors of GLS2 to clarify its unique roles in cancer cell metabolism.

Introduction

Cancer cells have altered metabolic pathways to meet the increased energetic, biosynthetic, and redox demands of the proliferative state.¹⁻³ The Warburg effect is a metabolic change in cancer cells characterized by aerobic glycolysis and lactate production.⁴ The reliance of cancer cells on Warburg metabolism and other metabolic adaptations creates therapeutic opportunities to target these changes.² A recent report described a high-throughput phenotypic screen for compounds able to reverse the Warburg effect induced by depolymerized α/β tubulin, which blocks mitochondrial voltage-dependent anion channels (VDACs).⁵ VDACs are a family of β -barrel transmembrane proteins in the outer mitochondrial membrane that control the flow of key metabolic substrates such as ATP, ADP, and Pi across the membrane.⁶ VDAC closure by α/β tubulin induces Warburg-like metabolism including depolarized mitochondria (lowered membrane potential $\Delta\Psi$), enhanced glycolysis, and lactate production.⁶ The goal of the screen was to find mimics of the small molecule Erastin, which is known to reverse the closure of VDACs by tubulin, restoring mitochondrial membrane potential and decreasing lactate formation.⁷ The screen identified two compounds, X1 and X4, that mimicked the ability of Erastin to reverse Warburg metabolism induced by VDAC closure. X1 and X4 increased the mitochondrial membrane potential, decreased lactate production, as well as induced an increase in reactive oxygen species (ROS), which ultimately resulted in mitochondrial dysfunction and cell death. These latter effects were specific to cancer cell lines and reversed by addition of *N*-acetyl cysteine (Figure 1).^{6,8,9}

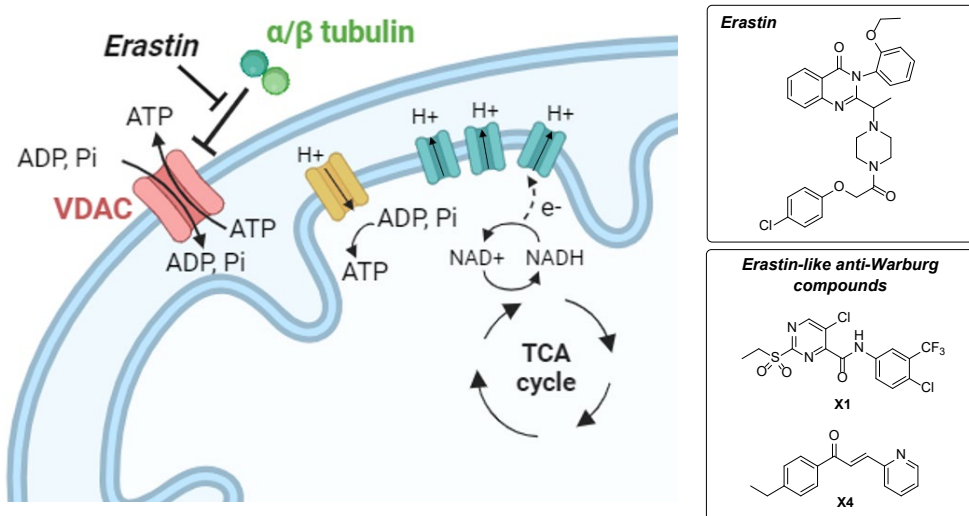


Figure 1. The voltage-dependent anion channels (VDACs) control the flow of anionic metabolites such as ATP and ADP across the outer mitochondrial membrane. Closure of VDACs by α/β tubulin induces glycolytic Warburg metabolism. Erastin blocks the closure of VDAC by tubulin and restores VDAC conductance. Erastin-like anti-Warburg compounds X1 and X1 were discovered in a phenotypic screen for the ability to similarly reverse Warburg metabolism resulting from tubulin-induced VDAC closure.

While the cellular effects of X1 and X4 were well-characterized in these studies, the target(s) of X1 and X4 were not identified. Compound X1 is a 2-sulfonyl pyrimidine, and has a similar structure to compound C9, a known inhibitor of glutaminase (GLS) enzymes (Figure 2A).¹⁰ Glutaminase is central to another common aspect of cancer cell metabolism; elevated glutamine uptake and metabolism.^{1,3,11–14} Glutamine is hydrolyzed to glutamate by the two glutaminase isozymes (GLS1 and GLS2), and the resulting glutamate serves as an anaplerotic TCA cycle input by subsequent oxidative deamination to α -ketoglutarate.^{11,14,15} Glutamate generated by GLS enzymes also supports the import of cystine through the system Xc- antiporter. Cystine is used in the biosynthesis of the antioxidant glutathione, necessary to manage the increased oxidative stress in cancer cells (Figure 2B).^{14,16}

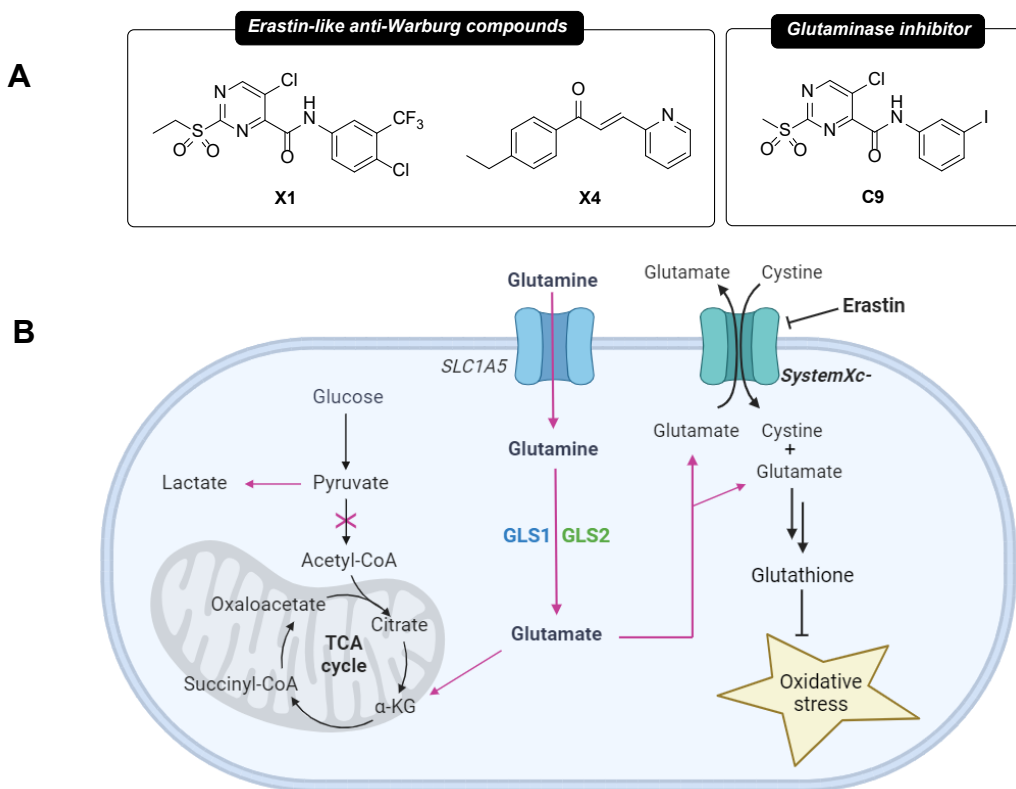


Figure 2. A) The Erastin-like anti-Warburg compound X1 is structurally similar to the known glutaminase inhibitor C9. **B)** Glutaminase enzymes GLS1 and GLS2 hydrolyze glutamine to glutamate, which supports glycolytic Warburg metabolism by TCA cycle anaplerosis. GLS-derived glutamate is also coupled to the import of cystine through system Xc⁻ which is required for the biosynthesis of the antioxidant glutathione. Erastin targets system Xc⁻ in addition to VDACs, so glutaminase inhibition may mimic the cellular effects of Erastin.

The cellular effects of the Erastin-like anti-Warburg compounds X1 and X4 are consistent with glutaminase as their target.^{11,14} Glutaminase inhibition can explain the anti-Warburg effects of compounds X1 and X4 by blocking the use of glutamine as an anaplerotic TCA cycle input. Glutaminase inhibition can also explain the observed increase in reactive oxygen species induced by X1 and X4 by suppressing the biosynthesis of glutathione. Importantly, in addition to targeting VDACs, Erastin also inhibits the system Xc⁻ antiporter; so glutaminase inhibition may well mimic the cellular effects of Erastin.¹⁷ As such, we wanted to evaluate glutaminase as a target of X1 and X4.

Additionally, X1 and X4 are electrophiles and may interact covalently with their cellular target(s). X4 is an aza-chalcone, a cysteine-reactive electrophile of the Michael acceptor class.¹⁸ X1 is a 2-sulfonyl pyrimidine, a less common electrophile known to react with cysteine by

nucleophilic aromatic substitution (S_NAr) (Figure 3).¹⁹ 2-Sulfonyl pyrimidines are the electrophile of covalent inhibitors of bacterial Sortase A and *S. mansoni* thioredoxin glutathione reductase.^{20,21} 2-Sulfonyl pyrimidines are also the electrophile in covalent probes that target cysteine residues of mutant p53.²²

We sought to determine if glutaminase is a target of X1 and X4, and if so, whether they act by a covalent mechanism. Glutaminase enzymes are known to be susceptible to inhibition by nonspecific cysteine-reactive electrophiles, including *N*-ethyl maleimide²³ and iodobutyltriphenylphosphonium (IBTP) salts.²⁴

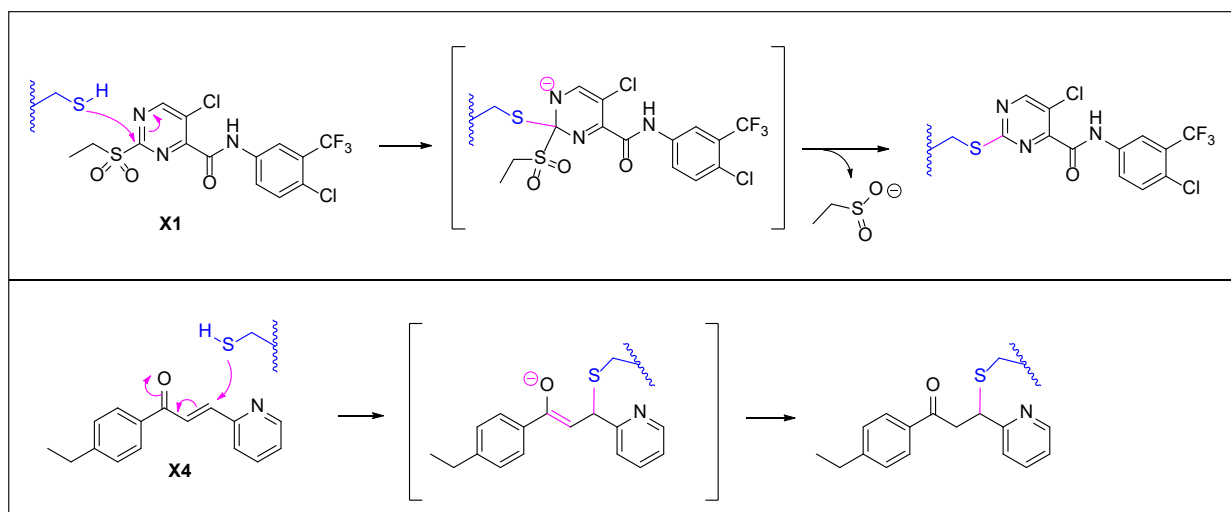


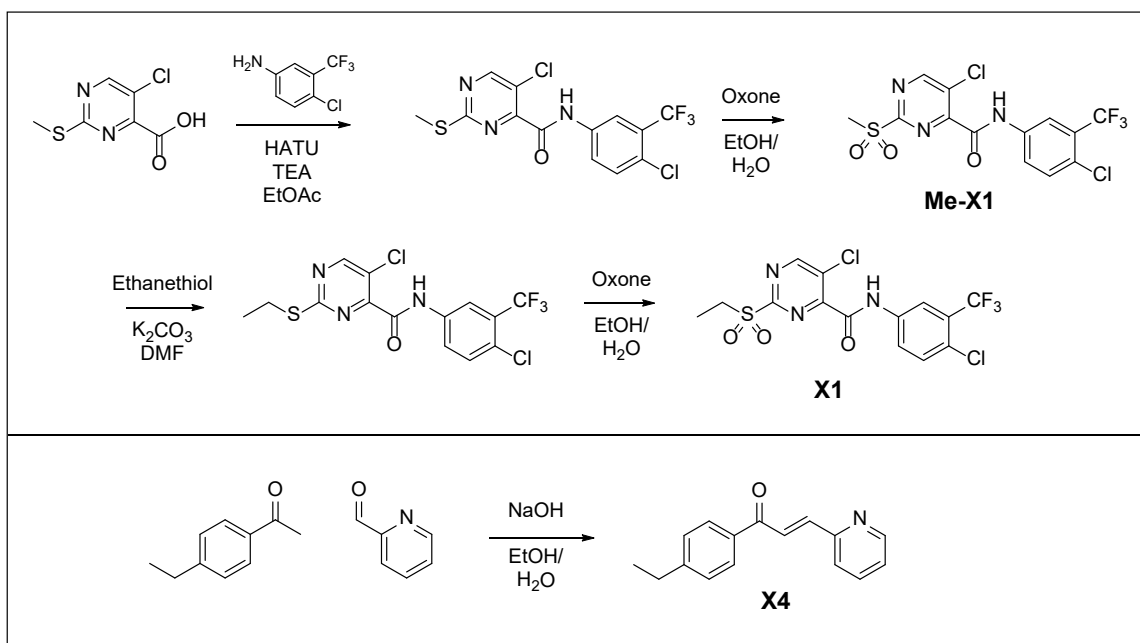
Figure 3. X1 is a 2-sulfonyl pyrimidine, an electrophile known to react with cysteine by a nucleophilic aromatic substitution (S_NAr) reaction. X4 is an electrophile of the Michael acceptor class, known to react with cysteine by conjugate addition.

Results

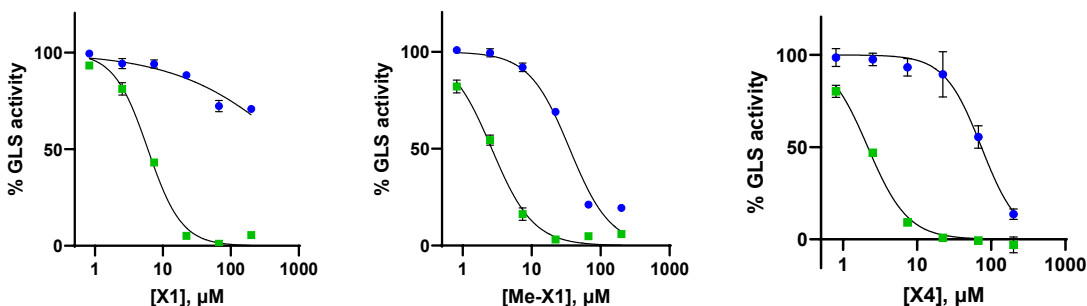
Compounds X1 and X4 are GLS2-selective glutaminase inhibitors.

We synthesized X1 and X4 according to Scheme 1 and evaluated them as inhibitors of GLS1 and GLS2. We also evaluated the methyl sulfone (Me-X1) intermediate along the X1 synthetic route due to its close similarity to the known glutaminase inhibitor C9. Because the potency of covalent inhibitors depends on both the inhibitor concentration and the incubation time with the enzyme, we tested X1 and X4 for inhibition of GLS1 and GLS2 with a significant fixed enzyme-inhibitor preincubation period before initiating the reaction by the addition of the glutamine substrate and phosphate, an activator of GLS activity.^{25–27} We used a 7-minute

preincubation period for the 2-sulfonyl pyrimidines X1 and Me-X1 and a 30-minute preincubation period for the aza-chalcone X4 reflecting the higher cellular potency of X1 compared to X4.⁵ The data show that X1, Me-X1, and X4 and were indeed glutaminase inhibitors, and all three are selective for the GLS2 isozyme (Figure 4). The data also show that Me-X1 was a better inhibitor of both GLS1 and GLS2 than X1, giving some preliminary insight into the structure-activity relationship of 2-sulfonyl pyrimidine inhibition of glutaminase.



Scheme 1. Chemical synthesis of the 2-sulfonyl pyrimidine compounds X1 and Me-X1 as well as the aza-chalcone X4.



| Compound | Structure | IC ₅₀ (μM) | | Enzyme-inhibitor preincubation time |
|----------|-----------|-----------------------|-----------|-------------------------------------|
| | | GLS1 | GLS2 | |
| X1 | | >200 | 6.0 ± 0.6 | 7 minutes |
| Me-X1 | | 35 ± 6 | 2.6 ± 0.4 | 7 minutes |
| X4 | | 73 ± 9 | 2.1 ± 0.2 | 30 minutes |

Figure 4. Dose-response curves of X1, Me-X1, and X4 inhibition of GLS1 (blue circles) and GLS2 (green squares) carried out with a fixed enzyme-inhibitor preincubation time. Summary of fixed-preincubation time IC₅₀ values derived from the [inhibitor] vs. normalized response - variable slope function of Graphpad Prism.

Compounds X1 and X4 are covalent glutaminase inhibitors.

We next tested if X1 and X4 are covalent glutaminase inhibitors. Specific covalent inhibitors act by a two-step mechanism; a reversible noncovalent binding step followed by a time-dependent covalent bond forming step.^{28,29} This mechanism makes the amount of enzyme inhibition by covalent inhibitors dependent on both the inhibitor concentration and the degree of time the enzyme is exposed to the inhibitor.^{30,31} We tested whether glutaminase inhibition by X1 and X4 shows such time-dependence by fixing the inhibitor concentration and varying the inhibitor-enzyme preincubation time before initiating the reaction by addition of glutamine substrate and phosphate activator. If the covalent inhibitor concentration is >10-fold higher than the enzyme concentration, the decay of enzyme activity should fit to a first-order decay rate

equation.^{28–30} Our data show that inhibition of GLS2 by X1 and X4 increased with increasing preincubation time, and the data fit well to a first-order decay rate equation, consistent with covalent inhibition (Figure 5A). We also tested for covalent inhibition by incubating X1 or X4 with GLS2 for 0 minutes or 30 minutes, subjecting the mixture to gel filtration to remove unattached X1 or X4 from the enzyme, followed by measuring the amount of active GLS2 enzyme in the eluent. With no incubation time, X1 and X4 could be separated from GLS2 by gel filtration; the recovered enzymatic activity was comparable to treating GLS2 with DMSO solvent. However, when X1 or X4 were incubated with GLS2 for 30 minutes before gel filtration, no enzyme activity was recovered, consistent with covalent attachment of X1 and X4 to GLS2 (Figure 5B). Together, these results suggest that X1 and X4 are covalent glutaminase inhibitors.

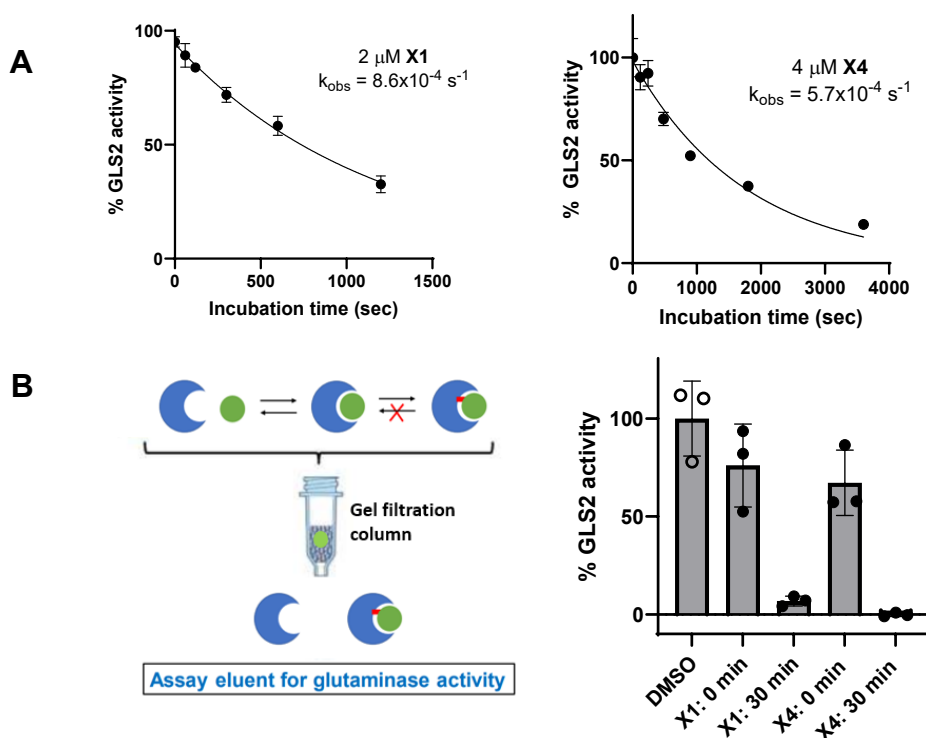


Figure 5. A) Time-dependent inhibition curves of GLS2 treated with X1 (2 μM) and X4 (4 μM) for increasing preincubation times before initiating the enzymatic reaction by addition of glutamine and phosphate. Curve fitting to obtain k_{obs} values was done using Graphpad Prism one-phase decay equation, plateau = 0. **B)** GLS2 was treated with X1 (10 μM) or X4 (20 μM) for either 0 minutes or 30 minutes, then subjected to a gel-filtration spin column to remove free X1 or X4 from the enzyme. The eluent was assayed for glutaminase activity.

k_{inact}/K_I of X1 and X4 against GLS1 and GLS2

The potency and selectivity of covalent enzyme inhibitors is best measured by $k_{\text{inact}}/K_{\text{I}}$ values rather than IC_{50} values. The $k_{\text{inact}}/K_{\text{I}}$ measurement captures both the concentration-dependence and time-dependence of the inhibitor's ability to inactivate the enzyme.^{28–31} Specific covalent inhibitors act by a two-step mechanism, with an initial noncovalent binding step followed by covalent bond formation. The k_{inact} is the first order rate constant of covalent bond formation of the enzyme-inhibitor complex, while K_{I} is the inhibitor concentration that gives an observed rate constant k_{obs} of enzyme inactivation that is $\frac{1}{2} k_{\text{inact}}$. The $k_{\text{inact}}/K_{\text{I}}$ ratio is thus a measure of the overall potency of a covalent inhibitor accounting for both its affinity for the recognition pocket as well as the rate of covalent bond formation.^{28–31}

We measured the $k_{\text{inact}}/K_{\text{I}}$ values for X1 and X4 against GLS1 and GLS2 using the k_{obs} method.^{28,29} This method involves measuring the first order decay rate constant of enzymatic activity (k_{obs}) for a series of inhibitor concentrations, then plotting k_{obs} vs the inhibitor concentrations (Figure 6). The plot of k_{obs} versus $[I]$ can be a hyperbolic curve, which indicates a two-step mechanism and allows individual determination of both k_{inact} and K_{I} . The plot of k_{obs} versus $[I]$ can also yield a straight-line, where the slope is $k_{\text{inact}}/K_{\text{I}}$. A straight line plot indicates either a one-step inhibition mechanism (with no noncovalent binding between the inhibitor and enzyme) or a two-step mechanism where the K_{I} value is higher than the highest inhibitor concentrations for which a k_{obs} value was obtained (indicating weak noncovalent binding).^{28–30} $k_{\text{inact}}/K_{\text{I}}$ values can be compared to k_{chem} , the second order rate constant for the reaction of free thiol nucleophiles with the inhibitor's electrophile. The k_{chem} value for the 2-sulfonyl pyrimidine electrophile of X1 has been reported to be between $0.1\text{--}0.5 \text{ M}^{-1}\text{s}^{-1}$ with glutathione and cysteine derivatives; indicating it is a fairly unreactive electrophile.^{19,32} An activity-based protein profiling study of simple 2-sulfonyl pyrimidines showed no protein labeling in cells, further demonstrating the low inherent reactivity of this electrophile.³³ The trans-chalcone electrophile of X4 has a somewhat higher inherent reactivity, with a reported k_{chem} of $3.0 \text{ M}^{-1}\text{s}^{-1}$ with the free thiol cysteamine.¹⁸

Our data show that X1 is a moderately potent covalent GLS2 inhibitor with a $k_{\text{inact}}/K_{\text{I}}$ value of $549 \text{ M}^{-1}\text{s}^{-1}$ and a poor inhibitor of GLS1 with a $k_{\text{inact}}/K_{\text{I}}$ value of $41 \text{ M}^{-1}\text{s}^{-1}$ (Table 1). This 13-fold selectivity of X1 for GLS2 over GLS1 is consistent with the observed selectivity measured using IC_{50} values with a fixed preincubation time. The plot of k_{obs} vs $[X1]$ for GLS1 was hyperbolic, which allowed for determination of k_{inact} and K_{I} individually ($K_{\text{I}} = 43 \mu\text{M}$; $k_{\text{inact}} = 1.8 \times 10^{-3} \text{ s}^{-1}$). This is evidence of a two-step mechanism; that high concentrations of X1 can saturate a specific binding

site on GLS1. The k_{obs} vs [X1] plot for GLS2 was linear, showing that there is either a one-step inhibition mechanism (no non-covalent binding between X1 and GLS2) or that the X1 concentrations used in the assay were substantially lower than the K_i value. The highest concentration of X1 for which a k_{obs} value was obtainable for GLS2 was 20 μM , which is less than half the K_i value X1 has for GLS1, so a two-step mechanism is possible. X1 showed a substantial “selectivity index”; its k_{inact}/K_i for GLS2 is >1000-fold higher than its relatively low k_{chem} value for free thiols such as glutathione and cysteine.^{19,32}

Our data show that X4 is a modestly potent GLS2 inhibitor with a k_{inact}/K_i value of 194 $\text{M}^{-1}\text{s}^{-1}$ and a very poor inhibitor of GLS1 with a k_{inact}/K_i value of 6.5 $\text{M}^{-1}\text{s}^{-1}$ (Table 1). X4 is a ~3-fold less potent GLS2 inhibitor than X1, which agrees with our fixed time point IC_{50} measurement and also aligns well with the relative cellular potencies reported for X1 and X4.^{5,8} The k_{obs} vs [X4] plot for both GLS1 and GLS2 was linear, showing that X4 either acts by a one-step inhibition mechanism (with no non-covalent binding between X4 and either enzyme) or the X4 concentrations used in the assay were substantially lower than its K_i value. X4 had a lower “selectivity index” than X1; the k_{inact}/K_i of X4 inhibition of GLS2 was 65-fold higher than its k_{chem} value for free thiols.¹⁸ The k_{inact}/K_i of X4 inhibition of GLS1 was only 2-fold greater than its k_{chem} value for free thiols; a difference so small that X4 may be considered to act by nonspecific alkylation of GLS1.

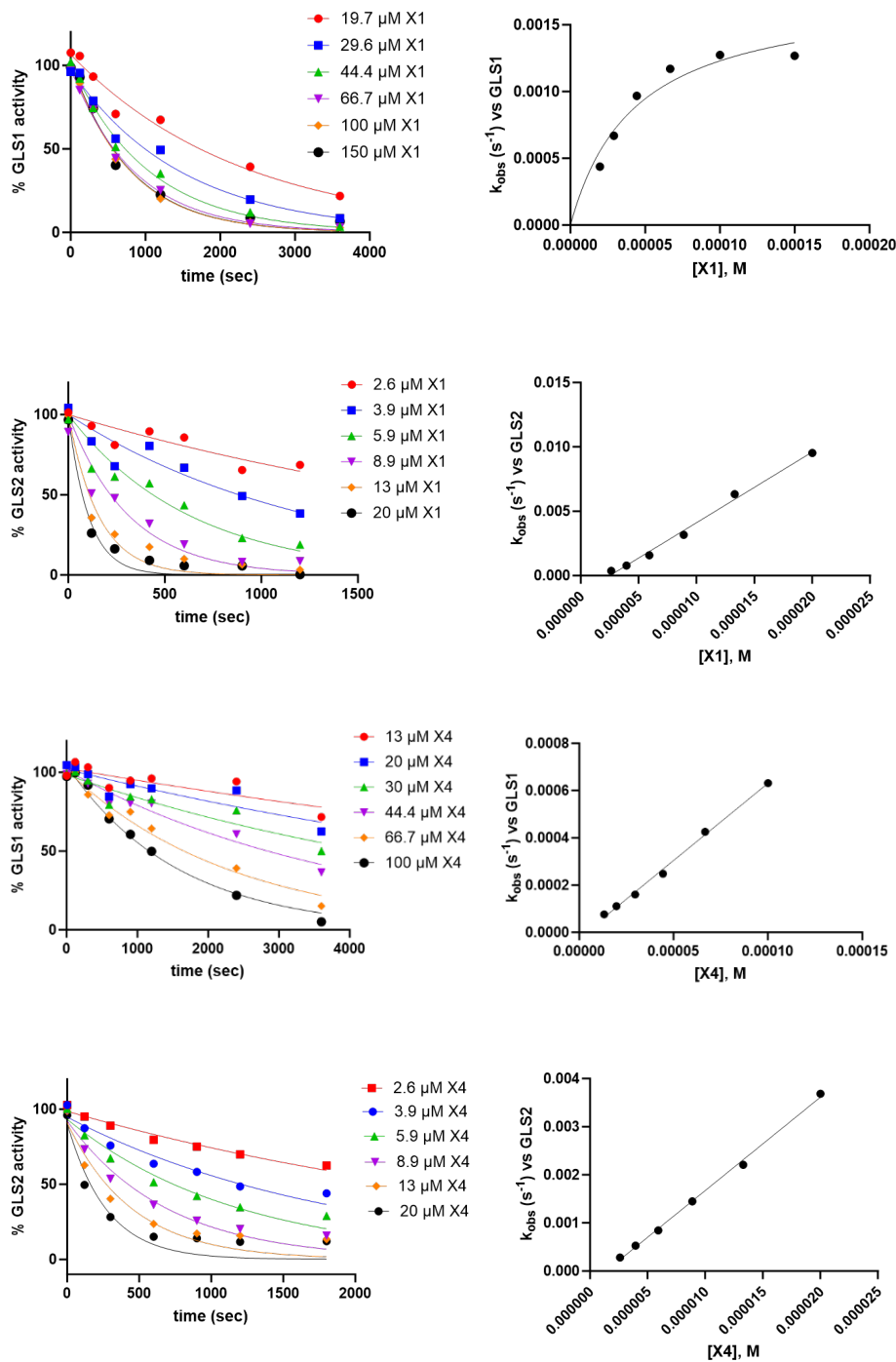


Figure 6. Left: Plots of GLS1 or GLS2 activity vs enzyme-inhibitor preincubation times for various X1 and X4 concentrations. Curve fitting to obtain k_{obs} values was done using GraphPad Prism one-phase decay equation, plateau = 0. **Right:** Plots of k_{obs} vs inhibitor concentration to obtain k_{inact}/K_I values either by simple linear regression or fitting the equation $Y = k_{inact} * X / (K_I + X)$ in GraphPad Prism.

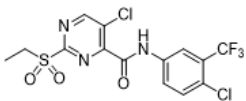
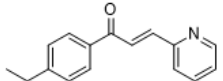
| Compound | Structure | k_{inact}/K_i ($\text{M}^{-1}\text{s}^{-1}$) | | k_{chem} vs free thiols ($\text{M}^{-1}\text{s}^{-1}$) |
|----------|---|---|--------------|---|
| | | GLS1 | GLS2 | |
| X1 |  | 41 ± 5 | 549 ± 23 | $0.1\text{-}0.5^{\text{a}}$ |
| X4 |  | 6.5 ± 0.5 | 194 ± 5 | 3.0^{b} |

Table 1. Summary of k_{inact}/K_i values for X1 and X4 inhibition of GLS1 and GLS2. ^{a,b}Literature k_{chem} values; see text for references.

Compounds X1 and X4 may interact with GLS2 in distinct ways

Early work on glutaminase inhibitors identified two related electrophilic glutamine analogs, 6-diazo-5-oxo-*L*-norleucine (DON) and *L*-2-amino-4-oxo-5-chloropentanoic acid, that are covalent glutaminase inhibitors targeting the active site serine.^{34,35} Despite their structural similarities, the rates of glutaminase inactivation by each compound had opposite responses to phosphate (the activator of glutaminase enzymatic activity)²⁵ being present during the inhibitor-enzyme incubation period. Inhibition of glutaminase by DON was found to require the presence of phosphate, while inhibition of glutaminase by *L*-2-amino-4-oxo-5-chloropentanoic acid was blocked by the presence of phosphate.^{34,35}

We tested whether GLS2 inactivation by X1 and X4 also responded differently to the presence of phosphate during the inhibitor-enzyme preincubation period. We generated dose-response curves of GLS2 inhibition by X1 and X4 with fixed preincubation times with either no phosphate or saturating concentrations of phosphate (100 mM) present during the preincubation period. We found that phosphate had no effect on the inhibition of GLS2 by X1, but phosphate did have a modest effect on the inhibition of GLS2 by X4, increasing its IC_{50} value 10-fold (Figure 7). Although the effect is small, this indicates that X1 and X4 likely interact with GLS2 differently; they either bind separate sites or occupy the same site with different poses.

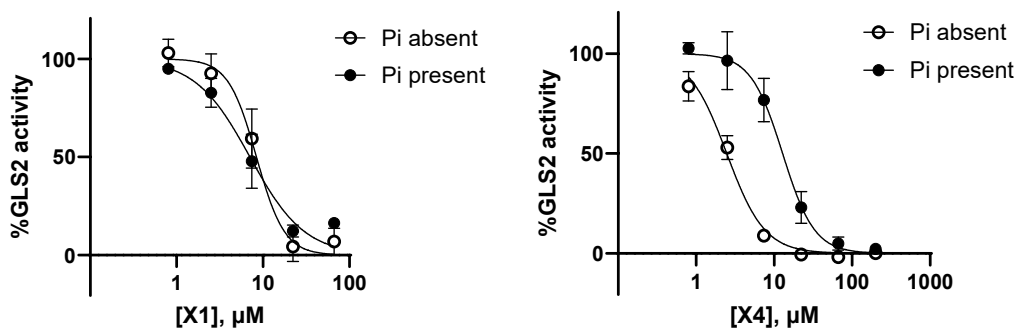


Figure 7. Dose-response curves of X1 and X4 inhibition of GLS2 with or without 100 mM phosphate present during the fixed enzyme-inhibitor preincubation period (7 minutes for X1, 30 minutes for X4).

Discussion

Here we show that X1 and X4, two compounds found in a phenotypic screen for Erastin-like anti-Warburg compounds, selectively target the GLS2 glutaminase isozyme. X1 is a 2-sulfonyl pyrimidine, like the known glutaminase inhibitor C9. X4 is an aza-chalcone, the first glutaminase inhibitor of this structural class. GLS1 is more commonly associated with cancer cells' elevated glutamine metabolism,^{11–14,36} so it is significant that the two most potent compounds identified in a phenotypic screen for anti-Warburg compounds are selective for GLS2. X1 and X4 are covalent glutaminase inhibitors. Previously reported covalent glutaminase inhibitors such as DON and related compounds are glutamine analogs that target other glutamine-utilizing enzymes, which is a significant liability.³⁶ The 2-sulfonyl pyrimidine and aza-chalcone classes of X1 and X4 are thus significant additions to covalent glutaminase inhibitors.

The reliance of cancer cells on glutamine and glutaminase activity has led to the discovery of many chemical inhibitors of glutaminase enzymes.^{11–14,36} Chief among these are compounds related to BPTES, a potent GLS1-specific inhibitor that binds at its dimer-dimer interface and stabilizes a catalytically inactive form of the enzyme.³⁷ Significant medicinal chemistry effort has focused this scaffold, resulting in many potent derivatives.^{38–40} One such analog CB-839 is in clinical trials, demonstrating that targeting glutaminase is widely viewed as a viable therapeutic strategy.⁴¹ GLS2-selective inhibitors are rare. The most prominent to date is the benzoquinone AV-1, which is ~8-fold selective for GLS2 over GLS1.⁴² X1 and X4 are thus significant additions to known GLS2-selective glutaminase inhibitors.

It is important to recognize the limitations of covalent probes to study cell and tissue biology.³¹ Covalent, time-dependent inhibitors such as X1 and X4 can lead to confounding results since the long incubation times typical for cell-based experiments can allow weaker targets such as GLS1 to be engaged. Compounds with 2-sulfonyl pyrimidine structures similar to X1 are known to covalently modify mutant p53, stabilizing its structure and rescuing its function. It is likely this allele is present in some cancer cell lines and could be engaged by X1.²²

The effects of X1 and X4 on cancer cell metabolism, mitochondrial function, and cell death due to oxidative damage have been well characterized.^{5,6,8,9,43} The cellular effects of X1 and X4 can now be attributed, at least in part, to GLS2 inhibition. GLS2 remains an enigmatic enzyme, with demonstrated roles as both a tumor promotor and tumor suppressor.^{14,15,44,45} X1 and X4 could be considered “pathfinder” compounds³¹ that may yield increasingly potent and selective GLS2 inhibitors upon further development. Such compounds will be useful tools to clarify the unique roles of GLS2 in cancer cell metabolism.

Acknowledgments

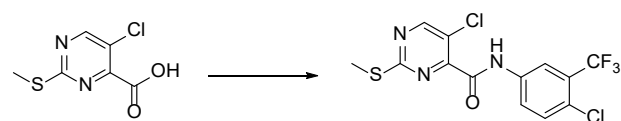
We thank the Ithaca College Summer Scholars program for funding summer research stipends for R.I., N.P.S., and S.J. We thank Rick Cerione and members of the Cerione lab particularly Thuy-Tien Thi Nguyen and William Katt for helpful discussions, advice, and reagents.

Experimental methods

General

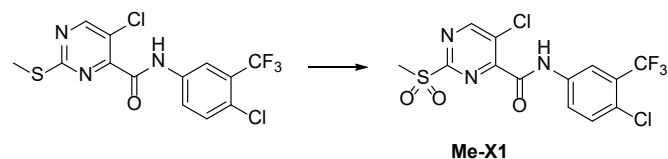
Nuclear magnetic resonance spectra were recorded on a JEOL ECX400 spectrometer. Glutaminase assays were measured on a Tecan Infinite M Nano spectrophotometer. Reagents and solvents for chemical synthesis were used without additional purification unless otherwise noted. Plasmids for the expression of 6-His tagged GLS1 (residues 72 to 598) cloned into pQE80 and human GLS2 (residues 38–602) cloned into pET28a were kind gifts of the Cerione laboratory at Cornell University.

Chemical synthesis



5-Chloro-2-(methylthio)pyrimidine-4-carboxylic acid (0.50 g, 2.4 mmol) was suspended in 10 mL of ethyl acetate, and triethylamine (0.68 mL, 4.9 mmol), HATU (0.93 g, 2.45 mmol), and 5-amino-2-chlorobenzotrifluoride (0.47 g, 2.4 mmol) were added sequentially and the reaction mixture was capped and stirred at room temperature overnight. The mixture was diluted with an additional 15 mL of ethyl acetate, and the organic layer was then washed with saturated solutions of ammonium chloride, sodium bicarbonate, and sodium chloride (20 mL each). The solution was dried over magnesium sulfate, filtered, and the solvent removed by rotary evaporation. The crude product was purified by silica gel chromatography using a gradient of 0-50 % ethyl acetate in hexane as the eluent to yield the product as a white solid (0.61 g, 65%).

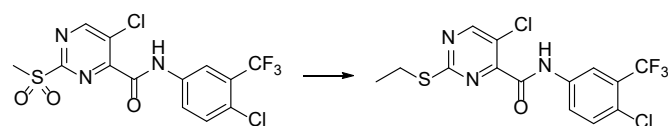
^1H NMR (400 MHz, CDCl_3): δ 9.75 (br s, 1H), 8.71 (s, 1H), 8.07 (d, $J = 2.3$ Hz), 7.89 (dd, 1H, $J = 8.7$ Hz, 2.3 Hz), 7.50 (d, 1H, $J = 8.7$ Hz), 2.63 (s, 3H). ^{13}C NMR (100 MHz, CDCl_3): δ 170.19, 161.25, 159.34, 150.36, 135.79, 132.27, 129.11 (q, $J = 31.8$ Hz) 127.90, 125.47, 123.91, 121.19, 119.06 (q, $J = 5.7$ Hz), 14.80.



The methyl thioether from the previous reaction (0.73 g, 1.9 mmol) was suspended in 30 mL of a 1:1 mixture of ethanol:water and cooled on ice. Oxone (2.35 g, 3.82 mmol) was added in portions

with stirring. The reaction mixture was allowed to warm to room temperature and stirred overnight. The reaction mixture was extracted with dichloromethane (4 x 10 mL) the combined organic layers was dried over magnesium sulfate, filtered, and the solvent removed by rotary evaporation. The crude product was purified by silica gel chromatography using a gradient of 0-50% ethyl acetate in dichloromethane as the eluent to yield the Me-X1 product as a white solid (0.45 g, 57%).

^1H NMR (400 MHz, DMSO- D_6): δ 11.41 (s, 1H), 9.45 (s, 1H), 8.23 (d, 1H, $J = 2.4$ Hz), 7.97 (dd, 1H, $J = 8.8$ Hz, 2.3 Hz), 7.76 (d, 1H, $J = 8.8$ Hz), 3.49 (s, 3H). ^{13}C NMR (100 MHz, DMSO- D_6): δ 163.30, 161.37, 161.16, 157.68, 137.59, 133.11, 130.84, 127.41, 126.34, 125.57, 124.45, 121.73, 119.31 (q, $J = 6$ Hz), 39.91.



The methyl sulfone from the previous reaction (0.45 g, 1.09 mmol) was dissolved in DMF (5 mL) and K_2CO_3 (0.45 g, 3.26 mmol) and ethanethiol (81 μL , 1.09 mmol) were added sequentially. The reaction mixture was capped and stirred at room temperature overnight. Water (10 mL) was added, and the thick precipitate was filtered and purified by silica gel chromatography using a gradient of 0-50% ethyl acetate in hexane as the eluent to yield the product as a white solid (0.29 g, 67%).

^1H NMR (400 MHz, CDCl_3): δ 9.76 (s, 1H), 8.70 (s, 1H), 8.07 (d, 1H, $J = 2.4$ Hz), 7.87 (dd, 1H, $J = 8.8$ Hz, 2.4 Hz), 7.50 (d, 1H, $J = 8.8$ Hz), 3.19 (q, 2H, $J = 7.2$ Hz), 1.44 (t, 3H, $J = 7.2$ Hz). ^{13}C NMR (100 MHz, CDCl_3): δ 169.90, 161.29, 159.34, 150.47, 135.81, 132.28, 129.32, 129.01, 127.87, 125.41, 123.86, 119.03 (q, $J = 5.8$ Hz), 26.09, 14.24.

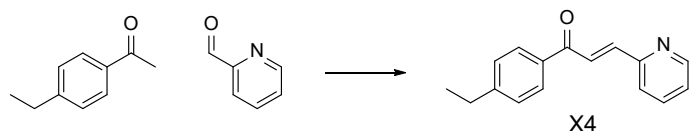


The ethyl thioether from the previous reaction (0.29 g, .73 mmol) was dissolved in acetonitrile (7 mL) with diethylamine (15 μL , 0.014 mmol). A solution of oxone (990 mg, 1.61 mmol) dissolved in water (10 mL) was added dropwise to the acetonitrile solution and stirred at room temperature overnight. The reaction mixture was then diluted with water (10 mL) and extracted with dichloromethane (5 x 10 mL). The pooled organic layers were dried over magnesium sulfate, filtered and the solvent removed by rotary evaporation. The crude product was purified by silica

gel chromatography using a gradient of 0-50 % ethyl acetate in dichloromethane as the eluent to yield X1 as a white solid (0.18 g, 57%).

^1H NMR (400 MHz, DMSO- D_6): δ 11.40 (s, 1H), 9.45 (s, 1H), 8.21 (d, 1H, J = 2.3 Hz), 7.97 (dd, 1H, J = 9.1 Hz, 2.3 Hz), 7.74 (d, 1H, J = 9.1 Hz), 3.67 (q, 2H, J = 7.3 Hz), 1.25 (t, 3H, J = 7.3 Hz).

^{13}C NMR (100 MHz, DMSO- D_6): δ 162.51, 161.37, 161.18, 158.07, 137.58, 133.08, 130.92, 127.43 (q, J = 30 Hz), 126.35, 125.53, 123.08 (q, J = 271 Hz), 119.31 (q, J = 5.8 Hz), 46.11, 7.06.



2-Pyridine carboxaldehyde (0.72 g, 6.7 mmol, 2.0 eq) was dissolved in 10 mL of a 4:1 water: methanol mixture and cooled on ice. Sodium hydroxide (0.13 g, 3.3 mmol, 1.0 eq) was added followed by dropwise addition of 4-ethyl acetophenone (0.50 g, 3.3 mmol, 1.0 eq) then stirred at 4°C overnight. The reaction mixture was diluted with saturated ammonium chloride (10 mL) then extracted with ethyl acetate (2 x 15 mL). The combined extracts were dried over magnesium sulfate, filtered and the solvent removed by rotary evaporation. The reaction mixture was purified by column chromatography using hexane, 10:1 hexane: ethyl acetate, then 7:1 hexane:ethyl acetate as the eluent to yield X4 as a gold oil (0.42 g, 53 %).

^1H NMR (400 MHz, CDCl_3): δ d 8.65 (d, 1H, J = 4.4 Hz), 8.09 (d, 1H, J = 15.2 Hz), 8.01 (d, 2H, J = 8.0 Hz), 7.74 (d, 1H, J = 15.2 Hz), 7.69 (dd, 1H, J = 6.8 Hz, 1.2 Hz), 7.44 (d, 1H, J = 8 Hz), 7.29 (d, 2H, J = 8.0 Hz), 7.25 (m, 1H), 2.69 (q, 2H, J = 7.6 Hz), 1.24 (t, 3H, J = 7.6 Hz). ^{13}C NMR (100 MHz, CDCl_3): δ 190.03, 153.36, 150.23, 142.49, 136.99, 135.56, 129.09, 128.28, 125.66, 125.48, 124.46, 29.08, 15.31.

Expression and purification of GLS1 and GLS2

Plasmids for the expression of 6-His tagged GLS1 (residues 72 to 598) cloned into pQE80 and human GLS2 (residues 38–602) cloned into pET28a were kind gifts of the Cerione laboratory at Cornell University. Overnight cultures of BL21(DE3) strains carrying these plasmids were grown at 37°C overnight in LB supplemented with 100 $\mu\text{g}/\text{mL}$ kanamycin (GLS2) or 100 $\mu\text{g}/\text{mL}$ ampicillin (GLS1). These cultures were diluted 1:100 into 1 L of LB media with antibiotics and grown at 37°C with shaking at 225 rpm until the OD_{600} reached 0.6. IPTG was added to a final concentration of 0.5 mM and the cultures shaken at 17°C for 18 hours. The cells were harvested by centrifugation and stored at -80°C. The cell pellets were lysed in 15 mL B-PER complete (ThermoFisher)

supplemented with an EDTA-free protease inhibitor tablet (Roche) according to the manufacturer's instructions. The supernatant was applied to 1 mL of Ni:NTA resin (Thermo Scientific) prewashed with wash buffer (50 mM Tris pH 8.0, 500 mM NaCl) and rocked at 4°C for 20 minutes. The beads were transferred to a disposable column and drained. The bead bed was washed at 4°C with 30 mL of wash buffer and 20 mL of wash buffer supplemented with 10 mM imidazole. Protein was eluted into 1 mL fractions at 4°C with wash buffer supplemented with 300 mM imidazole. A 20 µL aliquot of each fraction was analyzed by SDS-PAGE. Fractions with pure protein were pooled and the buffer was changed to 20 mM Tris (pH 8.5), 120 mM NaCl using a PD-10 desalting column (Cytiva). The eluent was portioned into 250 µL aliquots, snap frozen in liquid nitrogen, and stored at -80° C.

Glutaminase enzymatic assay

Glutaminase enzyme was diluted in glutaminase buffer (65 mM Tris acetate pH 8.6, 0.2 mM EDTA) to a final concentration of 50 nM (GLS1) or 200 nM (GLS2). The enzyme solution was supplemented with 0.01% triton X-100 to suppress nonspecific enzyme inhibition by colloidal aggregates.⁴⁶ The enzyme solution (79 µL) was added to UV-transparent 96 well plates followed by the inhibitor solution in DMSO or DMSO itself (1 µL), mixed by gently pipetting up and down, then incubated for the indicated amount of time at room temperature. The glutaminase reaction was initiated by the addition of 20 µL of a solution of glutamine (100 mM) and K₂HPO₄ (500 mM), then mixed by gently pipetting up and down and incubated at room temperature for seven minutes. The reactions were quenched by addition of 10 µL of HCl (3 M). An aliquot (10 µL) of each quenched glutaminase reaction was added to 190 µL of a glutamate dehydrogenase reaction, which consisted of Tris-HCl (100 mM, pH 9.4), NAD⁺ (2 mM), glutamate dehydrogenase (2 µL of a 50% glycerol solution, ≥35 units/mg protein), and hydrazine (1 µL) then incubated at room temperature for 40 min. The absorbance at 340 nm was measured and converted to glutamate concentrations using the extinction coefficient for NADH 6220 M⁻¹ cm⁻¹.

Gel filtration spin column

GLS2 was diluted into GLS buffer (65 mM Tris pH 8.6, 0.2 mM EDTA) to a final concentration of 800 nM. The GLS2 solution was portioned into 30 µL aliquots that were treated with 1 µL of either DMSO, X1 (300 µM), or X4 (600 µM) and incubated for either 0 minutes or 30 minutes. A 25 µL portion of the mixture was then applied to a G-Biosciences SpinOUT GT-100 column pre-equilibrated with GLS buffer. A 25 µL portion of the eluent was then diluted to a final volume of 80 µL and assayed for glutaminase activity as described above.

References

- (1) Pavlova, N. N.; Thompson, C. B. The Emerging Hallmarks of Cancer Metabolism. *Cell Metab.* **2016**, *23*, 27–47. <https://doi.org/10.1016/j.cmet.2015.12.006>.
- (2) Xiao, Y.; Yu, T.-J.; Xu, Y.; Ding, R.; Wang, Y.-P.; Jiang, Y.-Z.; Shao, Z.-M. Emerging Therapies in Cancer Metabolism. *Cell Metab.* **2023**, *35* (8), 1283–1303. <https://doi.org/10.1016/j.cmet.2023.07.006>.
- (3) DeBerardinis, R. J.; Chandel, N. S. Fundamentals of Cancer Metabolism. *Sci. Adv.* **2016**, *2* (5), e1600200. <https://doi.org/10.1126/sciadv.1600200>.
- (4) Liberti, M. V.; Locasale, J. W. The Warburg Effect: How Does It Benefit Cancer Cells? *Trends Biochem. Sci.* **2016**, *41* (3), 211–218. <https://doi.org/10.1016/j.tibs.2015.12.001>.
- (5) DeHart, D. N.; Lemasters, J. J.; Maldonado, E. N. Erastin-Like Anti-Warburg Agents Prevent Mitochondrial Depolarization Induced by Free Tubulin and Decrease Lactate Formation in Cancer Cells. *SLAS Discov.* **2018**, *23* (1), 23–33. <https://doi.org/10.1177/2472555217731556>.
- (6) Heslop, K. A.; Milesi, V.; Maldonado, E. N. VDAC Modulation of Cancer Metabolism: Advances and Therapeutic Challenges. *Front. Physiol.* **2021**, *12*, 742839. <https://doi.org/10.3389/fphys.2021.742839>.
- (7) Yagoda, N.; Von Rechenberg, M.; Zaganjor, E.; Bauer, A. J.; Yang, W. S.; Fridman, D. J.; Wolpaw, A. J.; Smukste, I.; Peltier, J. M.; Boniface, J. J.; Smith, R.; Lessnick, S. L.; Sahasrabudhe, S.; Stockwell, B. R. RAS–RAF–MEK-Dependent Oxidative Cell Death Involving Voltage-Dependent Anion Channels. *Nature* **2007**, *447* (7146), 865–869. <https://doi.org/10.1038/nature05859>.
- (8) DeHart, D. N.; Fang, D.; Heslop, K.; Li, L.; Lemasters, J. J.; Maldonado, E. N. Opening of Voltage Dependent Anion Channels Promotes Reactive Oxygen Species Generation, Mitochondrial Dysfunction and Cell Death in Cancer Cells. *Biochem. Pharmacol.* **2018**, *148*, 155–162. <https://doi.org/10.1016/j.bcp.2017.12.022>.
- (9) Heslop, K. A.; Rovini, A.; Hunt, E. G.; Fang, D.; Morris, M. E.; Christie, C. F.; Gooz, M. B.; DeHart, D. N.; Dang, Y.; Lemasters, J. J.; Maldonado, E. N. JNK Activation and Translocation to Mitochondria Mediates Mitochondrial Dysfunction and Cell Death Induced by VDAC Opening and Sorafenib in Hepatocarcinoma Cells. *Biochem. Pharmacol.* **2020**, *171*, 113728. <https://doi.org/10.1016/j.bcp.2019.113728>.
- (10) E. Costa, R. K.; Rodrigues, C. T.; H. Campos, J. C.; Paradela, L. S.; Dias, M. M.; Novaes da Silva, B.; de Valega Negrao, C. von Z.; Gonçalves, K. de A.; Ascensão, C. F. R.; Adamoski, D.; Mercaldi, G. F.; Bastos, A. C. S.; Batista, F. A. H.; Figueira, A. C.; Cordeiro, A. T.; Ambrosio, A. L. B.; Guido, R. V. C.; Dias, S. M. G. High-Throughput Screening Reveals New Glutaminase Inhibitor Molecules. *ACS Pharmacol. Transl. Sci.* **2021**, *4* (6), 1849–1866. <https://doi.org/10.1021/acsptsci.1c00226>.
- (11) Hensley, C. T.; Wasti, A. T.; DeBerardinis, R. J. Glutamine and Cancer: Cell Biology, Physiology, and Clinical Opportunities. *J. Clin. Invest.* **2013**, *123* (9), 3678–3684. <https://doi.org/10.1172/JCI69600>.
- (12) Nguyen, T.-T. T.; Katt, W. P.; Cerione, R. A. Alone and Together: Current Approaches to Targeting Glutaminase Enzymes as Part of Anti-Cancer Therapies. *Future Drug Discov.* **2022**, *4* (4), FDD79. <https://doi.org/10.4155/fdd-2022-0011>.
- (13) Yang, L.; Venneti, S.; Nagrath, D. Glutaminolysis: A Hallmark of Cancer Metabolism. *Annu. Rev. Biomed. Eng.* **2017**, *19* (1), 163–194. <https://doi.org/10.1146/annurev-bioeng-071516-044546>.
- (14) Yang, W.-H.; Qiu, Y.; Stamatatos, O.; Janowitz, T.; Lukey, M. J. Enhancing the Efficacy of Glutamine Metabolism Inhibitors in Cancer Therapy. *Trends Cancer* **2021**, *7* (8), 790–804. <https://doi.org/10.1016/j.trecan.2021.04.003>.

- (15) Katt, W. P.; Lukey, M. J.; Cerione, R. A. A Tale of Two Glutaminases: Homologous Enzymes with Distinct Roles in Tumorigenesis. *Future Med. Chem.* **2017**, *9* (2), 223–243. <https://doi.org/10.4155/fmc-2016-0190>.
- (16) Lewerenz, J.; Hewett, S. J.; Huang, Y.; Lambros, M.; Gout, P. W.; Kalivas, P. W.; Massie, A.; Smolders, I.; Methner, A.; Pergande, M.; Smith, S. B.; Ganapathy, V.; Maher, P. The Cystine/Glutamate Antiporter System x_c^- in Health and Disease: From Molecular Mechanisms to Novel Therapeutic Opportunities. *Antioxid. Redox Signal.* **2013**, *18* (5), 522–555. <https://doi.org/10.1089/ars.2011.4391>.
- (17) Dixon, S. J.; Patel, D. N.; Welsch, M.; Skouta, R.; Lee, E. D.; Hayano, M.; Thomas, A. G.; Gleason, C. E.; Tatonetti, N. P.; Slusher, B. S.; Stockwell, B. R. Pharmacological Inhibition of Cystine–Glutamate Exchange Induces Endoplasmic Reticulum Stress and Ferroptosis. *eLife* **2014**, *3*, e02523. <https://doi.org/10.7554/eLife.02523>.
- (18) Jackson, P. A.; Widen, J. C.; Harki, D. A.; Brummond, K. M. Covalent Modifiers: A Chemical Perspective on the Reactivity of α,β -Unsaturated Carbonyls with Thiols via Hetero-Michael Addition Reactions. *J. Med. Chem.* **2017**, *60* (3), 839–885. <https://doi.org/10.1021/acs.jmedchem.6b00788>.
- (19) Pichon, M.; Drelinkiewicz, D.; Lozano, D.; Moraru, R.; Hayward, L.; Jones, M.; Mccoy, M.; Allstrum-Graves, S.; Balourdas, D.-I.; Joerger, A.; Whitby, R.; Goldup, S.; Wells, N.; Langley, G.; Herniman, J.; Baud, M. 2-Sulfonylpyrimidines: Reactivity Adjustable Agents for Cysteine Arylation; preprint; Chemistry, 2023. <https://doi.org/10.26434/chemrxiv-2023-cx8vk>.
- (20) Lyu, H.; Petukhov, P. A.; Banta, P. R.; Jadhav, A.; Lea, W. A.; Cheng, Q.; Arnér, E. S. J.; Simeonov, A.; Thatcher, G. R. J.; Angelucci, F.; Williams, D. L. Characterization of Lead Compounds Targeting the Selenoprotein Thioredoxin Glutathione Reductase for Treatment of Schistosomiasis. *ACS Infect. Dis.* **2020**, *6* (3), 393–405. <https://doi.org/10.1021/acsinfecdis.9b00354>.
- (21) Barthels, F.; Meyr, J.; Hammerschmidt, S. J.; Marciniak, T.; Räder, H.-J.; Ziebuhr, W.; Engels, B.; Schirmeister, T. 2-Sulfonylpyrimidines as Privileged Warheads for the Development of *S. Aureus* Sortase A Inhibitors. *Front. Mol. Biosci.* **2022**, *8*, 804970. <https://doi.org/10.3389/fmolb.2021.804970>.
- (22) Bauer, M. R.; Joerger, A. C.; Fersht, A. R. 2-Sulfonylpyrimidines: Mild Alkylating Agents with Anticancer Activity toward P53-Compromised Cells. *Proc. Natl. Acad. Sci.* **2016**, *113* (36). <https://doi.org/10.1073/pnas.1610421113>.
- (23) Campos, J. A.; Aledo, J. C.; Del Castillo-Olivares, A.; Del Valle, A. E.; Núñez De Castro, I.; Márquez, J. Involvement of Essential Cysteine and Histidine Residues in the Activity of Isolated Glutaminase from Tumour Cells. *Biochim. Biophys. Acta BBA - Protein Struct. Mol. Enzymol.* **1998**, *1429* (1), 275–283. [https://doi.org/10.1016/S0167-4838\(98\)00240-4](https://doi.org/10.1016/S0167-4838(98)00240-4).
- (24) Smith, M. R.; Vayalil, P. K.; Zhou, F.; Benavides, G. A.; Beggs, R. R.; Golzarian, H.; Nijampatnam, B.; Oliver, P. G.; Smith, R. A. J.; Murphy, M. P.; Velu, S. E.; Landar, A. Mitochondrial Thiol Modification by a Targeted Electrophile Inhibits Metabolism in Breast Adenocarcinoma Cells by Inhibiting Enzyme Activity and Protein Levels. *Redox Biol.* **2016**, *8*, 136–148. <https://doi.org/10.1016/j.redox.2016.01.002>.
- (25) Nguyen, T.-T. T.; Ramachandran, S.; Hill, M. J.; Cerione, R. A. High-Resolution Structures of Mitochondrial Glutaminase C Tetramers Indicate Conformational Changes upon Phosphate Binding. *J. Biol. Chem.* **2022**, *298* (2), 101564. <https://doi.org/10.1016/j.jbc.2022.101564>.
- (26) Li, Y.; Erickson, J. W.; Stalneck, C. A.; Katt, W. P.; Huang, Q.; Cerione, R. A.; Ramachandran, S. Mechanistic Basis of Glutaminase Activation. *J. Biol. Chem.* **2016**, *291* (40), 11.
- (27) Ferreira, I. M.; Quesnay, J. E. N.; Bastos, A. C. S.; Rodrigues, C. T.; Vollmar, M.; Krojer, T.; Strain-Damerell, C.; Burgess-Brown, N. A.; von Delft, F.; Yue, W. W.; Dias, S. M. G.;

- Ambrosio, A. L. B. Structure and Activation Mechanism of the Human Liver-Type Glutaminase GLS2. *Biochimie* **2021**, *185*, 96–104.
- (28) Strelow, J. M. A Perspective on the Kinetics of Covalent and Irreversible Inhibition. *SLAS Discov.* **2017**, *22* (1), 3–20. <https://doi.org/10.1177/1087057116671509>.
- (29) Mons, E.; Roet, S.; Kim, R. Q.; Mulder, M. P. C. A Comprehensive Guide for Assessing Covalent Inhibition in Enzymatic Assays Illustrated with Kinetic Simulations. *Curr. Protoc.* **2022**, *2* (6), e419. <https://doi.org/10.1002/cpz1.419>.
- (30) Tonge, P. J. Quantifying the Interactions between Biomolecules: Guidelines for Assay Design and Data Analysis. *ACS Infect. Dis.* **2019**, *5* (6), 796–808. <https://doi.org/10.1021/acsinfecdis.9b00012>.
- (31) Hartung, I. V.; Rudolph, J.; Mader, M. M.; Mulder, M. P. C.; Workman, P. Expanding Chemical Probe Space: Quality Criteria for Covalent and Degradable Probes. *J. Med. Chem.* **2023**, *66* (14), 9297–9312. <https://doi.org/10.1021/acs.jmedchem.3c00550>.
- (32) Barthels, F.; Meyr, J.; Hammerschmidt, S. J.; Marciniak, T.; Räder, H.-J.; Ziebuhr, W.; Engels, B.; Schirmeister, T. 2-Sulfonylpyrimidines as Privileged Warheads for the Development of *S. Aureus* Sortase A Inhibitors. *Front. Mol. Biosci.* **2022**, *8*, 804970. <https://doi.org/10.3389/fmolb.2021.804970>.
- (33) Motiwala, H. F.; Kuo, Y.-H.; Stinger, B. L.; Palfey, B. A.; Martin, B. R. Tunable Heteroaromatic Sulfones Enhance In-Cell Cysteine Profiling. *J. Am. Chem. Soc.* **2020**, *142* (4), 1801–1810. <https://doi.org/10.1021/jacs.9b08831>.
- (34) Shapiro, R. A.; Clark, V. M.; Curthoys, N. P. Inactivation of Rat Renal Phosphate-Dependent Glutaminase with 6-Diazo-5-Oxo-L-Norleucine. Evidence for Interaction at the Glutamine Binding Site. *J. Biol. Chem.* **1979**, *254* (8), 2835–2838. [https://doi.org/10.1016/S0021-9258\(17\)30149-7](https://doi.org/10.1016/S0021-9258(17)30149-7).
- (35) Shapiro, R. A.; Clark, V. M.; Curthoys, N. P. Covalent Interaction of L-2-Amino-4-Oxo-5-Chloropentanoic Acid with Rat Renal Phosphate-Dependent Glutaminase. Evidence for a Specific Glutamate Binding Site and of Subunit Heterogeneity. *J. Biol. Chem.* **1978**, *253* (19), 7086–7090. [https://doi.org/10.1016/S0021-9258\(17\)38032-8](https://doi.org/10.1016/S0021-9258(17)38032-8).
- (36) Wang, Z.; Liu, F.; Fan, N.; Zhou, C.; Li, D.; Macvicar, T.; Dong, Q.; Bruns, C. J.; Zhao, Y. Targeting Glutaminolysis: New Perspectives to Understand Cancer Development and Novel Strategies for Potential Target Therapies. *Front. Oncol.* **2020**, *10*, 589508. <https://doi.org/10.3389/fonc.2020.589508>.
- (37) Robinson, M. M.; McBryant, S. J.; Tsukamoto, T.; Rojas, C.; Ferraris, D. V.; Hamilton, S. K.; Hansen, J. C.; Curthoys, N. P. Novel Mechanism of Inhibition of Rat Kidney-Type Glutaminase by Bis-2-(5-Phenylacetamido-1,2,4-Thiadiazol-2-Yl)Ethyl Sulfide (BPTES). *Biochem. J.* **2007**, *406* (3), 407–414. <https://doi.org/10.1042/BJ20070039>.
- (38) Thangavelu, K.; Pan, C. Q.; Karlberg, T.; Balaji, G.; Uttamchandani, M.; Suresh, V.; Schuler, H.; Low, B. C.; Sivaraman, J. Structural Basis for the Allosteric Inhibitory Mechanism of Human Kidney-Type Glutaminase (KGA) and Its Regulation by Raf-Mek-Erk Signaling in Cancer Cell Metabolism. *Proc. Natl. Acad. Sci.* **2012**, *109* (20), 7705–7710. <https://doi.org/10.1073/pnas.1116573109>.
- (39) Shukla, K.; Ferraris, D. V.; Thomas, A. G.; Stathis, M.; Duvall, B.; Delahanty, G.; Alt, J.; Rais, R.; Rojas, C.; Gao, P.; Xiang, Y.; Dang, C. V.; Slusher, B. S.; Tsukamoto, T. Design, Synthesis, and Pharmacological Evaluation of Bis-2-(5-Phenylacetamido-1,2,4-Thiadiazol-2-Yl)Ethyl Sulfide 3 (BPTES) Analogs as Glutaminase Inhibitors. *J. Med. Chem.* **2012**, *55* (23), 10551–10563. <https://doi.org/10.1021/jm301191p>.
- (40) McDermott, L. A.; Iyer, P.; Verneti, L.; Rimer, S.; Sun, J.; Boby, M.; Yang, T.; Fioravanti, M.; O'Neill, J.; Wang, L.; Drakes, D.; Katt, W.; Huang, Q.; Cerione, R. Design and Evaluation of Novel Glutaminase Inhibitors. *Bioorg. Med. Chem.* **2016**, *24* (8), 1819–1839. <https://doi.org/10.1016/j.bmc.2016.03.009>.

- (41) *Calithera* | *Glutaminase Inhibitor CB-839*. Calithera. <https://www.calithera.com/glutaminase-inhibitor-cb-839/> (accessed 2021-06-26).
- (42) Lee, Y.-Z.; Yang, C.-W.; Chang, H.-Y.; Hsu, H.-Y.; Chen, I.-S.; Chang, H.-S.; Lee, C.-H.; Lee, J.; Kumar, C. R.; Qiu, Y.-Q.; Chao, Y.-S.; Lee, S.-J. Discovery of Selective Inhibitors of Glutaminase-2, Which Inhibit mTORC1, Activate Autophagy and Inhibit Proliferation in Cancer Cells. *Oncotarget* **2014**, *5* (15), 6087–6101. <https://doi.org/10.18632/oncotarget.2173>.
- (43) Ventura, C.; Junco, M.; Santiago Valtierra, F. X.; Gooz, M.; Zhiwei, Y.; Townsend, D. M.; Woster, P. M.; Maldonado, E. N. Synergism of Small Molecules Targeting VDAC with Sorafenib, Regorafenib or Lenvatinib on Hepatocarcinoma Cell Proliferation and Survival. *Eur. J. Pharmacol.* **2023**, *957*, 176034. <https://doi.org/10.1016/j.ejphar.2023.176034>.
- (44) Gao, M.; Monian, P.; Quadri, N.; Ramasamy, R.; Jiang, X. Glutaminolysis and Transferrin Regulate Ferroptosis. *Mol. Cell* **2015**, *59* (2), 298–308. <https://doi.org/10.1016/j.molcel.2015.06.011>.
- (45) Lukey, M. J.; Cluntun, A. A.; Katt, W. P.; Lin, M. J.; Druso, J. E.; Ramachandran, S.; Erickson, J. W.; Le, H. H.; Wang, Z.-E.; Blank, B.; Greene, K. S.; Cerione, R. A. Liver-Type Glutaminase GLS2 Is a Druggable Metabolic Node in Luminal-Subtype Breast Cancer. *Cell Rep.* **2019**, *29* (1), 76-88.e7. <https://doi.org/10.1016/j.celrep.2019.08.076>.
- (46) McGovern, S. L.; Helfand, B. T.; Feng, B.; Shoichet, B. K. A Specific Mechanism of Nonspecific Inhibition. *J. Med. Chem.* **2003**, *46* (20), 4265–4272. <https://doi.org/10.1021/jm030266r>.